

# Electrode behaviors of Na-Zn liquid metal battery

Junli Xu<sup>1\*,3</sup>, Ana Maria Martinez<sup>2</sup>, Karen Sende Osen<sup>2</sup>, Ole Sigmund Kjos<sup>2</sup>, Ole Edvard Kongstein<sup>2</sup>, Geir Martin Haarberg<sup>3</sup>

1- School of Science, Northeastern University, Shenyang, 110004, China

2- SINTEF Materials and Chemistry, NO-7465 Trondheim, Norway

3- Department of Materials Science and Engineering, Norwegian University of Science and Technology, NO-7491 Trondheim, Norway

## Abstract

The electroreduction processes on a Mo electrode in a Na-Zn liquid metal battery cell with a molten NaCl-CaCl<sub>2</sub>-ZnCl<sub>2</sub> electrolyte were investigated at 565 °C. The effect of the battery operating parameters on the loss rate of Na was determined by using electrochemical techniques. The results indicated that the chemical reaction of the reduced Ca and Na with ZnCl<sub>2</sub> takes place very quickly, and the electroreduction of Zn (II) to Zn is controlled by mass-transfer. The diffusion coefficient of Zn (II) ions was found to be approximately  $3 \times 10^{-6}$  cm<sup>2</sup>/s. Moreover, **the results revealed that most of the reduced metals stick to the Mo electrode during charging. The increase of cell temperature and open-circuit time led to increase in the loss of Na. Volatilization is mainly responsible for the loss of Na, and a high current density during charging led to the severe competitive deposition of Zn with Na.**

**Keywords:** Liquid metal battery; electrochemistry; diffusion coefficient; coulombic efficiency;

---

E-mail: jlxu@mail.neu.edu.cn

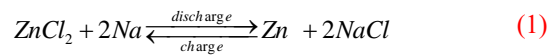
## 1. Introduction

Since the 1970s, Europe, the United States, and other developed countries have expedited their investigation into renewable energy sources because of the shortages of conventional energy sources and global environment stress. Solar and wind energy has particularly attracted significant attention because of the abundance of these natural sources. However, solar and wind are not constant and reliable sources of power in a grid as it is affected by weather. To overcome the intermittency of renewable energy production and maintain a constant power output, electrical energy storage (EES) is crucial [1, 2]. Currently mechanical, electrochemical, chemical, electrical, and thermal methods have been reported for storage of electric energy.

Meanwhile, with respect to broad market penetration, cost-effectiveness is probably the most important and fundamental issue of EES for a broad market penetration. Pumped-storage hydroelectricity is an economical route for large-scale energy storage. However, it requires special sites for energy storage. Previously, the use of rechargeable batteries in EES has been limited because of their relatively small capacity and high cost. Nevertheless, none of the existing technologies can offer sufficient flexible storage at a sufficient low cost.

In 2009, Sadoway proposed a molten salt battery known as a liquid metal battery, comprising three liquid layers as electroactive components. These liquid layers float over each other because of differences in their density and immiscibility. The all-liquid battery construction confers advantages of extremely high current density, long cycle life, and simple manufacture of large-scale storage systems [3, 4]. The Sadoway research group has developed several liquid metal batteries, such as Mg//Mg-Sb[5], Li//Sb-Pb [6], Li//Sb-Sn [7], calcium-based [8], and sodium-based liquid metal battery [9]. Among these reported liquid metal batteries, Li//Sb-Sn and Li//Sb-Pb batteries exhibit better properties with a flat discharge potential of approximately of 0.8V at 200-300 mA/cm<sup>2</sup> [6,7]. However, its self-discharge property has not been reported yet.

Recently, a new liquid metal battery was developed by the authors of this paper [11]. This battery employs liquid sodium and zinc as electrodes, with an equimolar mixture of CaCl<sub>2</sub> and NaCl as the electrolyte. During charging, Zn ( the positive electrode) loses electrons to form ZnCl<sub>2</sub> in the electrolyte, while Na<sup>+</sup> ions in the electrolyte get electrons forming Na metal as the negative electrode. The overall cell reaction for this Na-Zn liquid metal battery is as follows:



Zn could be co-deposited to a certain extent at the negative electrode during charging. The competitive deposition of Zn with Na can be restricted using an appropriate diaphragm and controlling the concentration of ZnCl<sub>2</sub> in the electrolyte. Even though Zn is produced at the Na electrode during charging, it sinks to the bottom, and may then be recovered in the Zn pool due to Na-Zn immiscibility at temperature greater than 556 °C.

In addition, Ca can be deposited at the negative electrode during charging. However, a eutectic 66.8 wt% CaCl<sub>2</sub> - 33.2 wt% NaCl electrolyte can be used to produce sodium by electrolysis. Only approximately 4 wt% of Ca has been reported to be deposited at the cathode in this mixture<sup>[10]</sup>. Moreover, even though Ca is deposited with Na at high current density during charging, it does not decrease the discharge property as Ca has a lower electrochemical equivalent compared to Na.

Meanwhile, the Na-Zn liquid metal battery can be assembled in the fully discharged state, which exhibits high safety as Na metal is not handled during assembly. The discharge flat voltage is greater than 1.5 V during discharge at 20 mA/cm<sup>2</sup>, while these values are approximately 1.0 V and 0.8 V during

discharge at 100 mA/cm<sup>2</sup> and 200 mA/cm<sup>2</sup> respectively as shown in Fig.1. Compared with the reported sodium zinc chloride batteries [12-14], sodium β" alumina solid electrolyte was substituted by molten CaCl<sub>2</sub>-NaCl mixture in our reported Na-Zn liquid metal battery, which make the battery more economical and increasing the possibility of charging and discharging at high current density. However, a severe self-discharge rate is a technical issue that needs to be addressed.

The self-discharge rate depends on the battery chemistry, electrode composition, current collector, electrolyte formulation, and storage temperature [15]. At a given temperature, there are three major contributions for the loss of Na. One is the dissolution of Na in the electrolyte. Na dissolves in NaCl-CaCl<sub>2</sub> electrolyte, forming Na<sup>+</sup> and releasing electrons. The excess electrons form so-called F-centers by occupying empty anion sites in the lattice. These electrons have high mobility, and a component of electronic conduction will be established. Another contribution for the loss of Na is its high sodium vapor pressure of Na at the operating temperature. High sodium vapor pressure leads to the loss of Na gas, which will not be in contact with the electrode and hence not available for the discharge reaction. Besides these factors, the reaction of Na with ZnCl<sub>2</sub> is mainly related to a high self-discharge rate. High concentration of zinc chloride in the electrolyte results in a high self-discharge rate. Moreover, a high zinc chloride concentration will lead to increased deposition of zinc instead of sodium, and decrease the cycle coulombic efficiency. As the concentration of zinc chloride in the electrolyte depends on the charging time, it is crucial to select an appropriate charging time at a certain current density to decrease the co-deposition of Zn with Na. Accordingly, the co-deposition of Zn with Na during charging in the Na-Zn liquid metal battery cell was investigated, and the effects of the battery parameters, such as cell temperature and charging time on the loss rate of Na were studied in this paper.

## 2. Experimental

The Na||Zn battery cell was assembled in an argon-filled glove box in the fully discharged state. A 1 mm Mo wire was used as negative electrode current lead, which was inserted approximately 2 cm into the electrolyte. NaCl-CaCl<sub>2</sub> (1:1 mole ratio) was used as the electrolyte. Zinc was placed at the bottom of the graphite cell with an Al<sub>2</sub>O<sub>3</sub> insulating sheath tube, and the NaCl-CaCl<sub>2</sub> salts were then added above the zinc. The cell was placed inside a quartz container and introduced in a vertical tube furnace attached to a glove box filled with Ar, and it was heated to 565 °C. Fig.2 shows the schematic cell used for electrochemistry tests.

All chemicals were dried before they were transferred into the glove box. NaCl (Alfa Aesar, 99.95 % purity) was dried at 120 °C for several days. CaCl<sub>2</sub> (Alfa Aesar, 99.95 % purity) was dried at 250 °C for 10 h. All tests were conducted at 560 °C using an Autolab/PGSTAT30 potentiostat controlled with GPES2 software. An Ag<sup>+</sup>/Ag (0.75mol of AgCl in the equimolar NaCl-CaCl<sub>2</sub> mixture) reference electrode was used for the electrode behavior studies. However, a Zn (II)/Zn reference electrode was used to investigate the competitive deposition of Zn with Na in NaCl-CaCl<sub>2</sub>- ZnCl<sub>2</sub> electrolyte as this reference electrode provides a well-defined zero for the potential scale. Zn (II)/Zn reference electrodes consisted of a pool of liquid zinc in an alumina tube. To avoid an undesirable junction potential, a slot was cut about 1 cm above the metal surface, which permitted the flow of the molten electrolyte into the alumina tube. A molybdenum wire was used as the electrical lead.

## 3. Results and discussion

Figure 3 shows the cyclic voltammograms obtained on Mo electrode in a fresh cell at different cathodic limits in the equimolar NaCl-CaCl<sub>2</sub> melt at 560 °C at a scan rate of 20 mV/s. As shown in Fig. 3, the

cathodic current density starts to increase after the potential reached -2.1 V vs. Ag<sup>+</sup>/Ag. However, no anodic peak at around -2.1 V was observed when the direction of the potential sweep was switched to positive before -2.2 V. A clear anodic peak was observed by switching the direction of potential sweep after -2.3 V. These results suggest that the deposition of Na or Ca metal starts at about -2.3 V. Moreover, as no reduction peak was observed before -2.3 V as shown in Fig. 3, no reduction process occurred before -2.3 V on the Mo wire in a fresh cell.

Figure 4 shows a cyclic voltammogram obtained for the Mo electrode in the NaCl-CaCl<sub>2</sub> bath at 560 °C at a scan rate of 100 mV/s after the cell was subjected to two charge-discharge cycles at 0.18 A. The cyclic voltammogram started at open circuit potential of -0.49 V, initially scanning in the cathodic direction.

Compared to that observed in Fig. 3, several new small cathodic peaks (peaks A, C1, C2 and C3) were observed at about -0.9 V, -1.9 V, -2.2 V and -2.4 V, respectively, and oxidation peaks were clearly observed during the anodic scan at -2.0 V (peak F), -1.8 V (peak D1) and -0.5 V (peak B) as shown in Fig. 4. The possible electrochemical reactions are summarized in Table 1. The standard electrode potentials were calculated by using the decomposition voltages of the corresponding chlorides. The Gibbs energies for calculating the potentials in the table were obtained using the thermodynamic software programme HSC. As shown in Table 1, the reduction potential of Zn<sup>2+</sup>/Zn is -0.65 V (vs. Ag<sup>+</sup>/Ag), while those of Na<sup>+</sup>/Na and Ca<sup>2+</sup>/Ca are very similar, corresponding to -2.58 and -2.59 V (vs. Ag<sup>+</sup>/Ag), respectively. By the comparison of the standard potentials with the cyclic voltammogram, it is reasonable to deduce that A and B peaks in Fig. 4 correspond to the Zn (II)/Zn electrochemical system, indicating that Zn (II) is not completely reduced to Zn during discharge. As the standard potentials of Ca<sup>2+</sup>/Ca and Na<sup>+</sup>/Na are quite close, both Ca and Na are most likely deposited at the same potential near -2.58 V vs. Ag<sup>+</sup>/Ag. Cathodic peaks C1, C2 and C3, which were observed at about -1.9 V, -2.2 V and -2.4 V, respectively, corresponded to the formation of the Ca-Zn alloy because of the immiscibility of Na and Zn at temperature greater than 556 °C. The potential for the deposition of Ca and Na metals after charge is more positive than that for the deposition of Ca and Na metal deposition before charging. The potential shift is related to the decrease of activity of metals (Ca and Na) during the deposition on a foreign substrate. Moreover, a small anodic peak at approximately 0.5 V was observed as shown in Fig. 4. This anodic peak may be caused by the anodic dissolution of Mo wire.

To investigate the competition of Zn (II) with Na<sup>+</sup> at different charge current densities, chronopotentiometry and chronoamperometry tests were carried out. Some ZnCl<sub>2</sub> was added into the cell, with an initial ZnCl<sub>2</sub> concentration of 1.91\*10<sup>-4</sup> mol/cm<sup>3</sup>, and the cell was subjected to several charge-discharge cycles before performing chronopotentiometry and chronoamperometry tests. Fig. 5 shows the typical chronopotentiometric curves for the Mo electrode during charging with different charge current densities. As shown in Fig. 5, when the applied current density is lower, there is a potential plateau at around -0.1 V vs. Zn<sup>2+</sup>/Zn, which is caused by the reduction of Zn (II) to Zn. This plateau potential is reduced with time which is caused by the lower Zn (II) concentration in solution as Zn is plated onto the negative electrode. Once the surface concentration of Zn (II) ions reaches zero, there is a sudden potential drop to a level corresponding to the reduction of Na<sup>+</sup> and/or Ca<sup>2+</sup>. The transition time became shorter with the increase of applied charge current. Moreover, other potential plateaus at around -0.8 V and -1.0 V were observed when the applied current density is less than 0.5 A/cm<sup>2</sup>. These potential plateau were not observed anymore when the applied current density was as high as 5 A/cm<sup>2</sup>. However, new potential plateaus at around -1.4 V and -1.7 V were observed under this high current density. These different potential plateaus

maybe caused by the different contents of Zn in the produced metals as the standard potential is about -1.9 V for Na<sup>+</sup>/Na or Ca<sup>2+</sup>/Ca vs. Zn<sup>2+</sup>/Zn as seen in Table 1.

The Sand's equation [16] is expressed as follows:

$$|I\tau^{1/2}| = \frac{nFD_0^{1/2}\pi^{1/2}C}{2} \quad (1)$$

where I is current density,  $\tau$  is the transition time, F is Faraday's constant, n is the number of electrons involved in the electron transfer reaction, C is the bulk concentration of the electroactive species, and D is its diffusion coefficient. The current density is linearly related to the inverse of the square root of time ( $\tau^{-\frac{1}{2}}$ ), and the diffusion coefficient of Zn (II) ions may be determined from the slope.

Moreover, the time dependence of the potential for a metal deposition is [17]:

$$E = E_{rev} + \frac{2.303RT}{nF} \log \frac{\tau^{\frac{1}{2}} - t^{\frac{1}{2}}}{\tau^{\frac{1}{2}}} \quad (2)$$

where  $E_{rev}$  is given by the Nernst equation. The number of electrons involved in the electron transfer reaction is readily calculated from the slope of the regression line according to the relation shown in equation (3).

$$n = \frac{2.303RT}{F \frac{dE}{d \log \frac{\tau^{\frac{1}{2}} - t^{\frac{1}{2}}}{\tau^{\frac{1}{2}}}}} \quad (3)$$

Figure 6 shows the relationship of the applied current density with  $\tau^{-\frac{1}{2}}$  which was obtained according to Fig. 5. It can be seen that the square root of the transition time linearly increased with the applied current density, and the diffusion coefficient of the Zn (II) ions was calculated as  $3.6 \times 10^{-6}$  cm<sup>2</sup>/s.

Figure 7 shows the plots of potential vs.  $-\log(\tau^{1/2}-t^{1/2})/\tau^{1/2}$ , and the number of electrons involved in the reduction process is readily calculated from the slope of the regression line. The time region used for the linear fit is on the interval of  $0.01\tau < t < 0.9\tau$ . The data of  $\tau$  and n obtained from the chronopotentiometry study (Fig. 5 and Fig. 7) are summarized in Table 2. These slopes gave  $n = 1.81 \pm 0.08$  for the number of electrons transferred in the overall electrode reaction, indicating that some Na co-deposited with Zn, and the ratio of plated Zn to Na is between 3 and 9 according to the n value listed in Table 2.

The major issue with chronopotentiometry lies in the accurate determination of the transition time. Hence, the diffusion coefficients are also determined using chronoamperometry. The chronoamperograms obtained show a constant current for the time values greater than 1s due to diffusion controlled process as shown in Fig. 8(a). The values of the diffusion coefficients obtained at various applied potentials can be determined by using Cottrell's equation as shown in equation (4). Fig. 8 (b) shows the plots of current density vs. the inverse of the square root of time, and the diffusion coefficient obtained by linear fitting at small value region of  $t^{-1/2}$  are summarized in Table 3. The average diffusion coefficient of the Zn(II) ion was calculated as  $3.0 \times 10^{-6}$  cm<sup>2</sup>/s. The value is 17% less than the value of  $3.6 \times 10^{-6}$  cm<sup>2</sup>/s obtained from the chronopotentiometry experiments.

$$I = \frac{nFD^{1/2}C}{\pi^{1/2}t^{1/2}} \quad (4)$$

As mentioned in the introduction, the high self-discharge rate of the battery is related to the loss of Na. The content of sodium can be measured by linear sweep voltammetry (LSV) after charging as the quantity of electricity (Q) for the oxidation process reflects the amount of metals which is electrodeposited and remained on the Mo electrode during charging. Fig. 9 shows the influence of charge time, charge current, temperature, and open circuit time on the quantity of oxidation electricity of Na and Zn ( $Q_{Na}$  and  $Q_{Zn}$ ).

Not all of Na was oxidized before the potential reached the Zn oxidation potential at a scan rate of 2 mV/s, while the Na and Zn oxidation peaks were completely separated at a scan rate of 1 mV/s as shown in Fig. 9(a). Therefore, when examining the effects of cell parameters on the contents of Na and Zn remained on the Mo electrode, experiments were carried out at a scan rate of 1 mV/s.

Fig. 9 (b) shows the LSV curves acquired on a Mo electrode under different experimental conditions (charging current, charging time, cell temperature, and open circuit time before doing LSV experiment). The quantities of electricity for the oxidation process of Na and Zn ( $Q_{Na}$  and  $Q_{Zn}$ ) obtained from Fig.9 (b) are summarized in Table 4. It could be seen that  $Q_{Na}$  and  $Q_{Zn}$  obtained from experiment (1) were both greater than those obtained from experiment (2) although the same coulombic during charge was input. The lower  $Q_{Na}$  of (2) is mainly related to the higher volatilization loss of Na with the increase of charging time. The higher  $Q_{Zn}$  of (1) revealed that a higher amount of Zn is deposited on the Mo electrode at a high current density because of the more rapid diffusion rate and content of Zn(II) at high current density during charging.

By comparing the results obtained from experiments (2) and (3), it was found that the  $Q_{Zn}$  in (3) was less than that in (2), which seems atypical as a higher amount of Zn should be deposited with the increase of charge time. This atypical character of  $Q_{Zn}$  was also observed via the comparison of the results of (3) and (4). Theoretically, the increase of open-circuit time leads to the increase of  $Q_{Zn}$  because of the prolonged chemical reaction of Na with  $ZnCl_2$ . The lower  $Q_{Zn}$  in these cases is possibly related to the accumulation of small Zn grains which possibly sink to the bottom of the cell.

Moreover, the increase of cell temperature leads to the rapid decrease of  $Q_{Na}$ , while  $Q_{Zn}$  was almost the same by the comparison of the results obtained from experiment (3) and (5), revealing that volatilization is the main reason for the loss of  $Q_{Na}$ . The selection of an appropriate electrolyte to decrease the operating cell temperature may be the main issue to be addressed in future studies.

In experiment (5), LSV was carried out using the same Mo wire electrode during charging, while the Mo wire was removed just after charging was completed, the finish of charge process, and a fresh Mo wire was inserted into the cell for the LSV experiments of (6). The data of  $Q_{Na}$  and  $Q_{Zn}$  obtained from experiment (6) were considerably less than those obtained from experiment (5), suggesting that most of the produced metal sticks to the Mo electrode. A bright gray metal was observed on the Mo wire surface after charging as shown in Fig. 10.

#### 4. Conclusions

Electrode reactions on a Mo electrode in a Na||Zn liquid metal battery cell with a molten NaCl-CaCl<sub>2</sub>-ZnCl<sub>2</sub> electrolyte were studied by electrochemical methods, and the following results were obtained.

- (1) The potential for the deposition of Ca and Na metals after charge is more positive than that for the deposition of Ca and Na metal deposition before charging. The potential shift is related to the decrease of the activity of metals (Ca and Na) during the deposition on a foreign substrate.

- (2) The electroreduction of Zn (II) ions is controlled by mass-transfer, while the reduction of Na<sup>+</sup> is controlled by charge-transfer in the equimolar NaCl- CaCl<sub>2</sub> molten salt mixture. The diffusion coefficient of Zn (II) ion is determined to be approximately  $3 \times 10^{-6}$  cm<sup>2</sup>/s.
- (3) Most of the reduced metals stick to the Mo electrode. The increase of cell temperature and open circuit time increase the loss of Na. **Volatilization is the main reason for the loss of Na, and higher current density of charge results in more severe co-deposition of Zn with Na during charge.**

### Acknowledgement

The authors gratefully acknowledge the financial support from the Norwegian Research Council.

### References

- [1] H. Chen, T. N. Cong, W. Yang, C. Tan, Y. Li, Y. Ding, Progress in electrical energy storage system: A critical review, *Progress in Natural Science*, 19 (2009) 291-312.
- [2] Z. Yang, J. Zhang, M. C. W. Kintner-Meyer, X. Lu, D. Choi, J. P. Lemmon, J. Liu, Electrochemical energy storage for green grid, *Chemical Reviews*, 111(2011) 3577-3613.
- [3] H. Kim, D. A. Boysen, J. M. Newhouse, B. L. Spatocco, B. Chung, P.J. Burke, D. J. Bradwell, K. Jiang, A. A. Tomaszowska, K. Wang, W. Wei, L.A. Ortiz, S. A. Barriga, S. M. Poizeau, and D. R. Sadoway, Liquid metal batteries: past, present, and future, *Chemical Reviews*, 113 (2013) 2075-2099.
- [4] H. Li, H. Yin, K. Wang, S. Cheng, K. Jiang, D. R. Sadoway, Liquid Metal Electrodes for Energy Storage Batteries, *Advanced Energy Materials*, 6(14) 1600483 (2016)
- [5] D. J. Bradwell, H. Kim, A. H. C. Sirk, D. R. Sadoway, Magnesium-antimony liquid metal battery for stationary energy storage, *Journal of the American Chemical Society*, 134 (2012) 1895-1897.
- [6] K. Wang, K. Jiang, B. Chung, T. Ouchi, P. J. Burke, D. A. Boysen, D. J. Bradwell, H. Kim, U. Muecke, D. R. Sadoway, Lithium-antimony-lead liquid metal battery for grid-level energy storage, *Nature*, 514(2014) 348-350.
- [7] H. Li, K. Wang, S. Cheng, K. Jiang, High performance liquid metal battery with environmentally friendly antimony-tin positive electrode, *ACS Applied Materials & Interfaces*, 8 (2016) 12830-12835.
- [8] H. Kim, D. A. Boysen, T. Ouchi, D. R. Sadoway, Calcium-bismuth electrodes for large-scale energy storage (liquid metal batteries), *Journal of Power Sources*, 241 (2013) 239-248.
- [9] Rakan F. Ashour, Huayi Yin, Takanari Ouchi, Douglas H. Kelley, Donald R. Sadoway, Molten Amide-Hydroxide-Iodide Electrolyte for a Low-Temperature Sodium-Based Liquid Metal Battery, *Journal of The Electrochemical Society*, 164 (2017) A535-A537.
- [10] D. Aurbach, *Nonaqueous Electrochemistry*, Marcel Dekker, New York, USA, 1999.
- [11] J. L. Xu, O. S. Kjos, K. S. Osen, A. M. Martinez, O. E. Kongstein, G. M. Haarberg, Na-Zn liquid metal battery, *Journal of Power Sources*, 332 (2016) 274-280.
- [12] P. Parthasarathy, N. Weber, A. V. Virkar, High temperature sodium-zinc chloride batteries with sodium beta"-alumina solid electrolyte (base), *ECS Transactions*, 6 (2007) 67-76.
- [13] H. T. Kim, S. I. Kim, H. L. Choi, W. Park, C. Kim, Effect of Zn/NaCl ratios on the charge/discharge performance in Na-ZnCl<sub>2</sub> battery, *Journal of the Korean Crystal Growth and Crystal technology*, 25(2015) 74-79.
- [14] X. Lu, G. Li, J. Y. Kim, J. P. Lemmon, V. L. Sprenkle, Z. Yang, A novel low-cost sodium-zinc chloride battery, *Energy & Environmental Science*, 6 (2013) 1837-1843.

- [15] N. Azimi, Z. Xue, N. D. Rago, C. Takoudis, M. L. Gordin, J. Song, D. Wang, Z. Zhang, Fluorinated Electrolytes for Li-S Battery: Suppressing the self-discharge with an electrolyte containing fluoroether solvent, *Journal of The Electrochemical Society*, 162 (2015) A64-A68.
- [16] Southampton electrochemistry group, *Instrumental methods in electrochemistry*, University of Southampton, 2001.
- [17] Trond Store, *Electrodeposition of metals from molten salts* (PhD thesis), Norwegian University of Science and Technology, 1999.